Neutron multiplicity measurements of Cf and Fm isotopes

Darleane C. Hoffman, G. P. Ford, J. P. Balagna, and L. R. Veeser
Los Alamos Scientific Laboratory, Los Alamos, New Mexico 87545
(Received 26 June 1979)

Prompt neutrons in coincidence with the fission fragments from the spontaneous fission of ^{250,252,254}Cf and ^{257}Fm were measured inside a 75-cm-diameter, Gd-loaded liquid scintillation counter having a neutron-detection efficiency of about 78%. Measurements for ^{256}Fm were done just outside the counter with an efficiency of 31%. The kinetic energies of both fission fragments and the number of neutrons for each fission event were recorded. From these data, the fragment kinetic energies and masses and the neutron multiplicity distributions were determined for ^{250,252,254}Cf and ^{257}Fm. Variances of neutron multiplicity distributions as a function of total fragment kinetic energy and the ratio of fragment masses have been calculated and are presented for all the nuclides studied.

[RADIOACTIVITY, FISSION ^{250,252,254}Cf, ^{257}Fm; measured neutron multiplicity distributions as a function of total kinetic energy and mass ratio. ^{256}Fm; measured average and variance of neutron multiplicity distributions as a function of total kinetic energy and mass ratio.]

INTRODUCTION

We first became interested in measuring the number of prompt neutrons emitted in spontaneous fission (SF) as a result of our early studies[1] of the mass distributions from SF of ^{257}Fm. A knowledge of prompt neutron emission $\bar{\nu}$ as a function of fragment mass and kinetic energy is necessary to obtain pre-neutron-emission mass-yield distributions from radiochemical or kinetic energy measurements of the fission products. The marked differences in the yields obtained for symmetric mass division of ^{257}Fm for different assumptions about the mass dependence of $\bar{\nu}$ were discussed in Ref. 1.

Information concerning the excitation or deformation energies of the fragments can also be deduced from studies of prompt neutron emission. In the case of the Fm isotopes, these quantities have turned out to be of particular interest because of the trend with increasing mass of the Fm isotopes toward symmetric mass division. This symmetric mass division is accompanied[1] by very high total kinetic energy (TKE) and by reduced neutron emission.[2] The average total neutron emission per fission event $\bar{\nu}_T$ for the low energy

TABLE I. Data for neutrons emitted in SF of Cf and Fm isotopes.

Nuclide	ν_T	$\sigma_{\nu_T}^2$	Γ_2
^{246}Cf	3.14 ± 0.09 [a]	1.66 ± 0.31 [a]	0.850 ± 0.031 [a]
^{250}Cf	3.50 ± 0.09 [b]		0.839 ± 0.002 [a]
	3.49 ± 0.04 [c]	1.49 ± 0.03 [c]	0.838 ± 0.001 [c]
^{252}Cf	3.735 ± 0.014 [d]	1.57 ± 0.01 [a]	0.845 ± 0.001 [a]
		1.55 ± 0.02 [c]	0.843 ± 0.001 [c]
^{254}Cf	3.89 ± 0.05 [b]		
	3.77 ± 0.05 [c]	1.56 ± 0.01 [c]	0.846 ± 0.006 [c]
^{254}Fm	3.96 ± 0.14 [a]	1.50 ± 0.02 [a]	0.843 ± 0.012 [a]
^{256}Fm	3.73 ± 0.18 [a]	2.30 ± 0.65 [a]	0.897 ± 0.047 [a]
		1.82 ± 0.08 [c]	0.863 ± 0.006 [c]
^{257}Fm	3.77 ± 0.02 [e]	2.49 ± 0.06 [e]	0.910 ± 0.002 [a]
	3.85 ± 0.05 [c]	2.51 ± 0.02 [c]	0.911 ± 0.001 [c]

[a] Reference 6.
[b] Data from Ref. 7 normalized to $\bar{\nu}_T = 3.735$ for ^{252}Cf.
[c] This work.
[d] Reference 5.
[e] Reference 2.

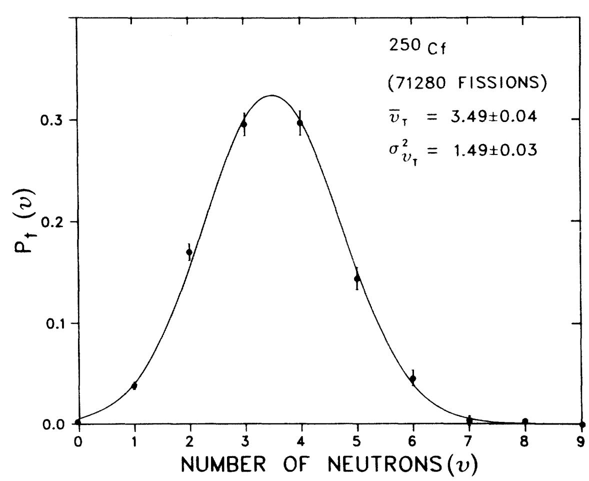

FIG. 1. The "unfolded" frequency distribution $P_t(\nu)$ for neutron emission from ^{250}Cf (SF). The standard deviation based on the number of events is shown for each point.

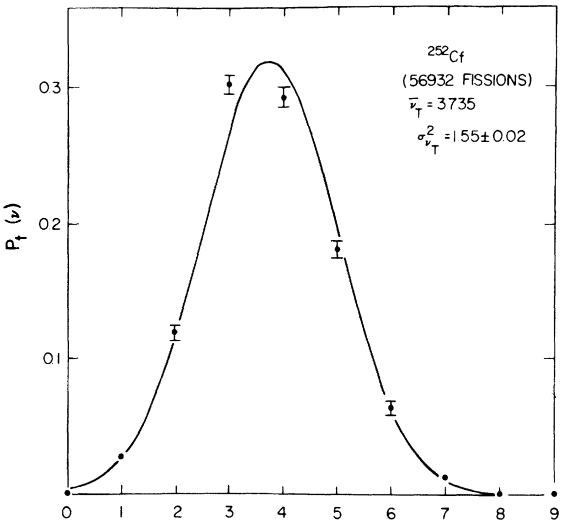

FIG. 2. Same as Fig. 1 for ^{252}Cf (SF).

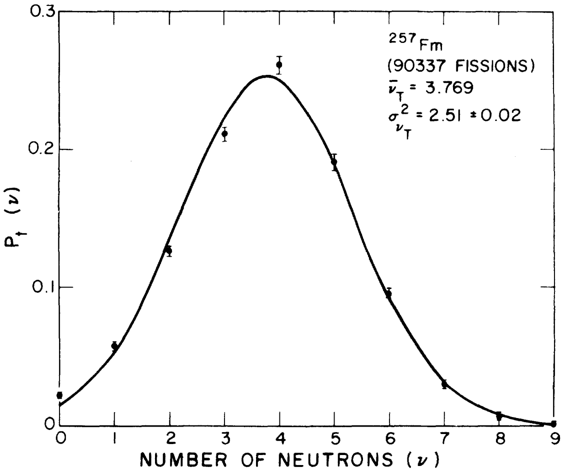

FIG. 4. Same as Fig. 1 for ^{257}Fm (SF).

fission of the heavier actinides generally increases[3] with Z and A. However, $\bar{\nu}_T$ does not increase with A for Fm isotopes, probably because the increased yield of symmetric mass division results in fragments which are closer to the doubly magic ^{132}Sn configuration. Thus the fragments may be more nearly spherical, resulting in a larger kinetic energy due to Coulomb repulsion, a lower fragment excitation energy, and lower neutron and/or photon emission from the fragments. Since our first measurements[2] of the prompt neutron emission in SF of ^{257}Fm, we have measured neutrons emitted from fission fragments of other spontaneously fissioning nuclides to look for changes in $\bar{\nu}$ as a function of TKE, mass split, and Z and A of the fissioning nucleus. The neutron multiplicity distributions $\bar{\nu}$ and variances for SF of ^{250}Cf, ^{252}Cf, ^{254}Cf, and ^{257}Fm, and $\bar{\nu}$ and variance for ^{256}Fm as a function of fragment kinetic energies and mass ratios are presented here.

EXPERIMENTAL

A 75-cm-diam spherical tank containing Nuclear Enterprise NE-323 liquid scintillator loaded with 0.5 wt% gadolinium was used in the current studies. The tank has a 15-cm-diam cylindrical hole through the center, in which was placed an evacuated chamber containing a pair of 200-mm^2 silicon surface-barrier detectors 1.5 cm apart facing each other. The appropriate SF source on a 40-

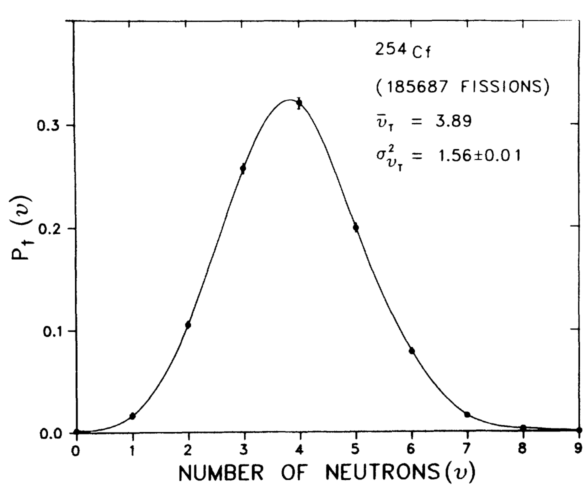

FIG. 3. Same as Fig. 1 for ^{254}Cf (SF).

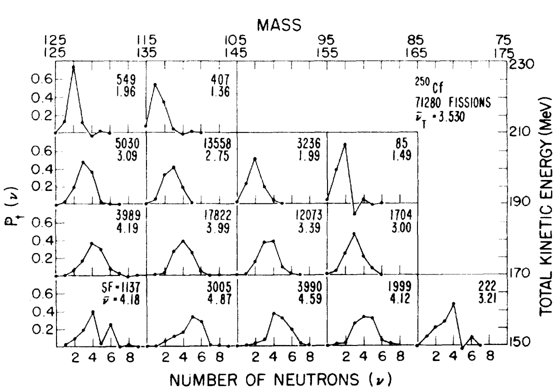

FIG. 5. $P_t(\nu)$ for ^{250}Cf as a function of TKE and fragment masses. Total number of fission events observed and $\bar{\nu}$ are shown for each group.

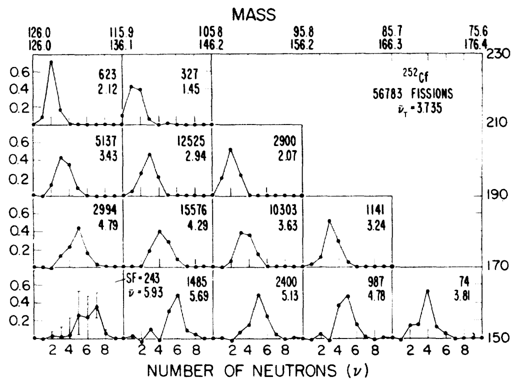

FIG. 6. Same as Fig. 5 for ^{252}Cf.

μg/cm^2 carbon or VYNS film was held equidistant between the detectors, giving a 20% detection efficiency for coincident fission fragments. In this arrangement, the neutrons emitted as a function of the kinetic energy of the fragments from the SF of ^{250}Cf, ^{252}Cf, ^{254}Cf, and ^{257}Fm were detected with an efficiency of about 78%. For ^{256}Fm, the evacuated chamber was placed so that the source was at the edge of the tank with one detector inside and the other just outside the tank; the resulting neutron-detection efficiency was 31%. The detection of coincident fission fragments triggered a 40-μs gate for the tank after a 1-μs delay to exclude prompt gamma rays from fission and recoil protons from thermalization of neutrons. The background was measured at regular intervals throughout these experiments by using a clock to start the gate at a rate typically several times the average fission rate. Details of the construction and operation of the tank have been given elsewhere.[4]

The ^{250}Cf, ^{252}Cf, and ^{257}Fm were produced by successive neutron capture in targets irradiated in the High Flux Isotope Reactor (HFIR), processed at the Oak Ridge National Laboratory, and made available to us under the Transplutonium Production Program of the Division of Research of the U. S. Department of Energy. The ^{257}Fm was further purified from rare earths and other actinides by elution from cation-exchange resin columns with ethanol-HCl and hot alpha-hydroxyisobutyrate solutions. Only relatively small samples of ^{257}Fm are available and the measurements were performed on sources of a few SF's per minute. The ^{250}Cf was prepared by neutron irradiation of ^{249}Bk in the HFIR to make ^{250}Bk which beta decayed to ^{250}Cf and was chemically separated from the target material. At the time of measurement the atom fraction of ^{250}Cf was 0.999. Of the total SF activity

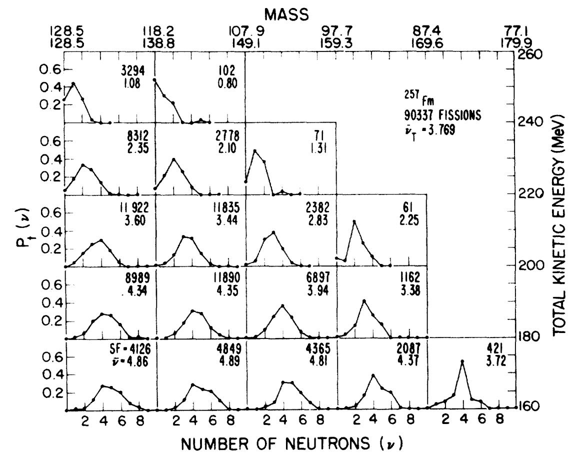

FIG. 8. Same as Fig. 5 for ^{257}Fm.

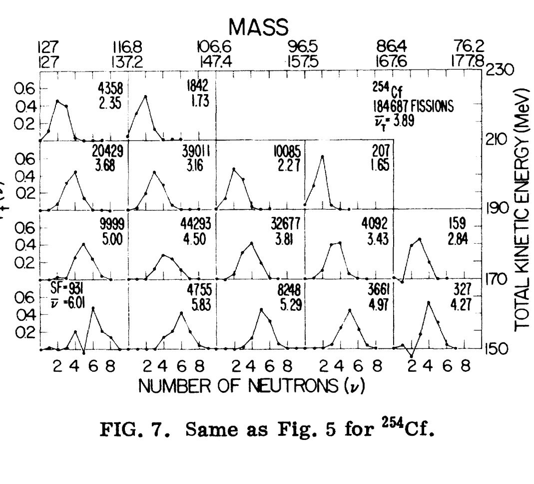

FIG. 7. Same as Fig. 5 for ^{254}Cf.

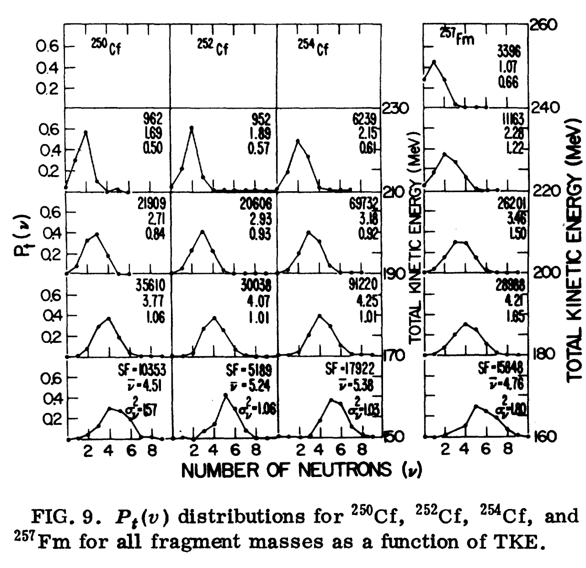

FIG. 9. $P_t(\nu)$ distributions for ^{250}Cf, ^{252}Cf, ^{254}Cf, and ^{257}Fm for all fragment masses as a function of TKE.

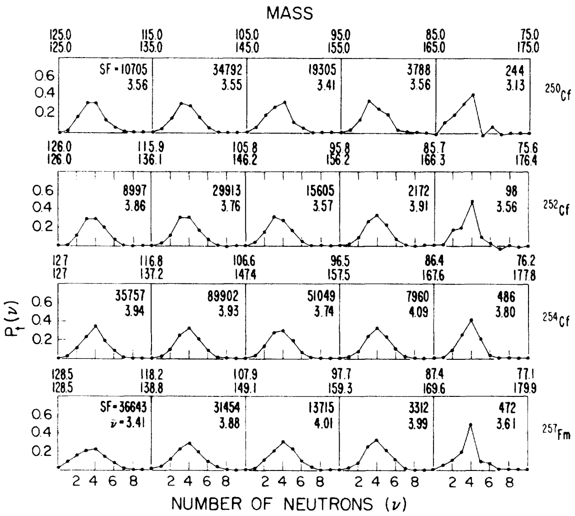

FIG. 10. $P_t(\nu)$ distributions for ^{250}Cf, ^{252}Cf, ^{254}Cf, and ^{257}Fm for all TKE's as a function of fragment masses.

of ≈100 SF/min, 83% was due to ^{250}Cf and the remainder to ^{252}Cf. The observed $\bar{\nu}_T$ and variance were corrected for this contribution from ^{252}Cf. The ^{254}Cf ($T_{1/2}$ = 60 d) and ^{256}Fm ($T_{1/2}$ = 2.6 h) were prepared by collection on carbon foils of products recoiling from triton irradiations of ^{254}Cf and ^{254}Es. The ^{254}Cf (≈60 SF/min) was self-transferred during irradiation of a ^{254}Cf target and the ^{256}Fm (≈6000 SF/min) was the result of beta decay of an ^{256}Es recoil source produced by the (t,p) reaction on ^{254}Es. These two sources were therefore essentially weightless. Standard sources of ^{252}Cf of several different strengths were prepared to approximate the samples being measured and were used to determine the neutron-detection efficiency.

RESULTS

In general, the object of these measurements was to obtain $\bar{\nu}$, σ_ν^2, and neutron multiplicity distribu-

TABLE II. Means and variances of neutron multiplicity distributions of ^{250}Cf (71 280 fission events).

	Mass numbers derived from mass ratios					
	125–135 125–115	135–145 115–105	145–155 105–95	155–165 95–85	165–175 85–75	All mass numbers
210–230 MeV						
SF[a]	549	407				962
$\bar{\nu}$	1.96	1.36				1.69 ± 0.04
σ_ν^2	0.33	0.50				0.50 ± 0.07
Γ_2	0.577	0.535				0.584 ± 0.030
190–210 MeV						
SF[a]	5 030	13 558	3 236	85		21 909
$\bar{\nu}$	3.09	2.75	1.99	1.49		2.71 ± 0.01
σ_ν^2	0.67	0.77	0.63	0.28		0.84 ± 0.02
Γ_2	0.747	0.738	0.657	0.453		0.745 ± 0.003
170–190 MeV						
SF[a]	3 989	17 822	12 073	1704	22	35 610
$\bar{\nu}$	4.19	3.99	3.39	3.00	2.26	3.77 ± 0.01
σ_ν^2	1.16	0.98	0.84	0.73	0.29	1.06 ± 0.02
Γ_2	0.827	0.811	0.778	0.748	0.615	0.809 ± 0.001
150–170 MeV						
SF[a]	1 137	3 005	3 990	1999	222	10 353
$\bar{\nu}$	4.18	4.87	4.59	4.12	3.21	4.51 ± 0.02
σ_ν^2	1.98	1.80	1.17	1.22	1.02	1.57 ± 0.04
Γ_2	0.874	0.871	0.838	0.829	0.787	0.855 ± 0.002
All energies						
SF[a]	10 705	34 792	19 305	3788	244	
$\bar{\nu}$	3.56	3.55	3.41	3.56	3.13	
σ_ν^2	1.40	1.52	1.51	1.38	1.03	
Γ_2	0.829	0.839	0.836	0.828	0.785	

[a]Number of fission events in the specified energy and mass ranges.

TABLE III. Means and variances of neutron multiplicity distributions of ^{252}Cf (56 932 fission events).

	Mass numbers derived from mass ratios					
	126.0–136.1 125.0–115.9	136.1–146.2 115.9–105.8	146.2–156.2 105.8–95.8	156.2–166.3 95.8–85.7	166.3–176.4 85.7–75.6	All mass numbers
210–230 MeV						
SF[a]	623	327				952
$\bar{\nu}$	2.12	1.45				1.89
σ_ν^2	0.35	0.68				0.57
Γ_2	0.606	0.633				0.630
190–210 MeV						
SF[a]	5137	12 525	2 900	44		20 606
$\bar{\nu}$	3.43	2.94	2.07 ± 0.02	1.71		2.93
σ_ν^2	0.73	0.79	0.68 ± 0.05	0.11		0.93
Γ_2	0.770	0.751	0.676 ± 0.012	0.454		0.767
170–190 MeV						
SF[a]	2994	15 576	10 303	1141	24	30 038
$\bar{\nu}$	4.79	4.29 ± 0.01	3.63	3.24	2.81	4.07
σ_ν^2	0.91	0.90 ± 0.03	0.75	0.62	0.93	1.01
Γ_2	0.831	0.816 ± 0.002	0.782	0.751	0.762	0.815
150–170 MeV						
SF[a]	243	1 485	2 400	987	74	5 189
$\bar{\nu}$	5.93 ± 1.15	5.69	5.13	4.78	3.81	5.24
σ_ν^2	1.44 ± 0.29	1.05	0.83	0.74	0.96	1.06
Γ_2	0.872 ± 0.009	0.857	0.837	0.823	0.804	0.848
All energies						
SF[a]	8997	29 913	15 605	2172	98	
$\bar{\nu}$	3.86	3.76	3.57	3.91	3.56	
σ_ν^2	1.50	1.53	1.55	1.33	1.14	
Γ_2	0.842	0.843	0.842	0.831	0.809	

[a]Number of fission events in the specified energy and mass ranges.

tions and variances as a function of TKE and fragment mass ratio, rather than to redetermine $\bar{\nu}_T$ for these nuclides. This necessitated making energy and neutron measurements of coincident fission fragments from sources on thin films over periods of several weeks in order to obtain statistically significant data from the low intensity sources. Concurrent measurements of ^{252}Cf sources could not be made in this physical arrangement although measurements of ^{252}Cf were made before and after each run to monitor the neutron-detection efficiency. (The resulting efficiency was 78.5 ± 1.0% based on $\bar{\nu}_T = 3.735$ for ^{252}Cf, Ref. 5.) Our values for $\bar{\nu}_T$ and $\sigma_{\nu_T}^2$ for ^{250}Cf, ^{254}Cf, and ^{257}Fm from our current experiments are given in Table I together with averages for these and other Cf and Fm isotopes calculated by Lazarev.[6] Our currently determined variances of 1.49 ± 0.03 for ^{250}Cf and 2.51 ± 0.02 for ^{257}Fm are in agreement with our earlier[2,6] reported measurements. Our value of 1.55 ± 0.02 for ^{252}Cf is in good agreement with the reported average[6] of previous values of 1.57 ± 0.01. No previous determination has been reported for ^{254}Cf, but our value of 1.56 ± 0.01 is essentially the same as that for ^{252}Cf. Our value of $\bar{\nu}_T$ of 3.49 ± 0.04 for ^{250}Cf was obtained after correction for the SF contribution from the ^{252}Cf in the sample. This correction decreased the measured value by only 1.2%. The quoted error of 0.04 arises principally from the standard deviation computed for several determinations of the neutron-detection efficiency measured with ^{252}Cf sources. (The statistical error of the ^{250}Cf measurement was only 0.006.) The value of $\bar{\nu}_T = 3.49 \pm 0.04$ is in excellent agreement with that of Orth[7] of 3.50 ± 0.09, obtained by renormalizing his reported value of $\bar{\nu} = 3.53 \pm 0.09$ to $\bar{\nu} = 3.735$ for ^{252}Cf.

Our $\bar{\nu}_T$ values of 3.77 ± 0.05 and 3.85 ± 0.05 for

TABLE IV. Means and variances of the neutron multiplicity distributions of ^{254}Cf (185 687 fission events).

	Mass numbers derived from mass ratios					
	127.0–137.2 127.0–116.8	137.2–147.3 116.8–106.7	147.3–157.5 106.7–96.5	157.5–167.6 96.5–86.4	167.6–177.8 86.4–76.2	All mass numbers
210–230 MeV						
SF[a]	4358	1842	39			6239
$\bar{\nu}$	2.35	1.73	0.62			2.15
σ_ν^2	0.49	0.58	0.37			0.61
Γ_2	0.663	0.617	0.356			0.668
190–210 MeV						
SF[a]	20429	39011	10085	207		69732
$\bar{\nu}$	3.68	3.16	2.27	1.65		3.18
σ_ν^2	0.71	0.77	0.57	0.43		0.92
Γ_2	0.780	0.761	0.670	0.553		0.776
170–190 MeV						
SF[a]	9999	44293	32677	4092	159	91220
$\bar{\nu}$	5.00	4.50	3.81	3.43	2.84	4.25
σ_ν^2	0.89	0.88	0.73	0.68	0.45	1.01
Γ_2	0.836	0.821	0.787	0.766	0.704	0.821
150–170 MeV						
SF[a]	931	4755	8248	3661	327	17922
$\bar{\nu}$	6.01	5.83	5.29	4.97	4.27	5.38
σ_ν^2	1.84	1.03	0.76	0.81	0.49	1.03
Γ_2	0.885	0.859	0.838	0.832	0.793	0.850
All energies						
SF[a]	35757	89902	51049	7960	486	
$\bar{\nu}$	3.94	3.93	3.74	4.09	3.80	
σ_ν^2	1.55	1.53	1.52	1.47	0.93	
Γ_2	0.846	0.845	0.841	0.843	0.801	

[a]Number of fission events in the specified energy and mass ranges.

^{254}Cf and ^{257}Fm, respectively, are in reasonable agreement with the earlier determinations given in Table I. Again, the quoted error arises primarily from the uncertainty in the efficiency. Due to the relatively long measurement times and the absence of simultaneous efficiency monitoring, we have chosen to normalize our present data to the earlier values[7,2] of 3.89 ± 0.05 and 3.77 ± 0.02 for ^{254}Cf and ^{257}Fm, respectively.

The neutron multiplicity distributions associated with the SF of ^{250}Cf, ^{252}Cf, ^{254}Cf, and ^{257}Fm are shown in Figs. 1–4. These "unfolded" distributions were obtained from the observed frequency distributions by solving the equations,[2]

$$p_d(n) = \sum_{k=0}^{n} \sum_{\nu=n-k}^{\nu_{max}} \binom{\nu}{n-k} \epsilon^{n-k}(1-\epsilon)^{\nu-n-k} \times p_b(k) p_t(\nu), \quad n = 1, \ldots, \nu_{max} \tag{1}$$

where $p_d(n)$ is the probability of observing n events per fission, ϵ is the neutron-detection efficiency, $p_t(\nu)$ is the probability that ν neutrons are emitted per fission, and $p_b(k)$ is the probability of k background events in 40 μs. The maximum number of neutrons considered, ν_{max}, was 9. The background was found to follow the Poisson distribution $p_b(k) = e^{-a} a^k / k!$, where a is the average number of background events. The average background was 0.02 to 0.04 counts per 40-μs gate for most runs, but was 0.20 counts per gate for the ^{250}Cf measurement and 0.14 counts per gate for the ^{256}Fm measurement. The deadtime of 0.1 μs per pulse was neglected.

The quantity Γ_2, which is independent of the neutron-detection efficiency,[8] was calculated from the relationship,

$$\Gamma_2 = (\sigma_d^2 - \sigma_b^2 - \bar{\nu}_d + \bar{\nu}_b)(\bar{\nu}_d - \bar{\nu}_b)^{-2} + 1 , \tag{2}$$

where the subscripts d and b refer to the observed

TABLE V. Means and variances of neutron multiplicity distributions of ^{257}Fm (90 337 fission events).

	Mass numbers derived from mass ratios					
	128.5–138.8 128.5–118.2	138.8–149.1 118.2–107.9	149.1–159.3 107.9–97.7	159.3–169.6 97.7–87.4	169.6–179.9 87.4–77.1	All mass numbers
240–260 MeV						
SF[a]	3 294	102				3 396
$\bar{\nu}$	1.08	0.80				1.07
σ_ν^2	0.65	1.02				0.66
Γ_2	0.631	1.342				0.644
220–240 MeV						
SF[a]	8 312	2 778	71			11 163
$\bar{\nu}$	2.35	2.10	1.31			2.28
σ_ν^2	1.26	1.08	0.65			1.22
Γ_2	0.800	0.769	0.613			0.796
200–220 MeV						
SF[a]	11 922	11 835	2 382	61		26 201
$\bar{\nu}$	3.60	3.44	2.83	2.25		3.46
σ_ν^2	1.66	1.33	0.98	1.00		1.50
Γ_2	0.851	0.821	0.769	0.753		0.836
180–200 MeV						
SF[a]	8 989	11 890	6 897	1162	50	28 988
$\bar{\nu}$	4.34	4.35	3.94	3.38	2.68	4.21
σ_ν^2	1.82	1.61	1.31	1.18	0.79	1.65
Γ_2	0.866	0.855	0.831	0.807	0.737	0.855
160–180 MeV						
SF[a]	4 126	4 849	4 365	2087	421	15 848
$\bar{\nu}$	4.86	4.89	4.81	4.37	3.72	4.76
σ_ν^2	1.96	1.86	1.63	1.39	1.35	1.80
Γ_2	0.877	0.873	0.862	0.844	0.829	0.870
All energies						
SF[a]	36 643	31 454	13 715	3312	472	
$\bar{\nu}$	3.41	3.88	4.01	3.99	3.61	
σ_ν^2	2.75	2.12	1.84	1.59	1.39	
Γ_2	0.944	0.883	0.865	0.849	0.830	

[a]Number of fission events in the specified energy and mass ranges.

and background values, respectively. The calculated values for the overall distributions are given in Table I and are in good agreement with those from previous determinations.

In the case of ^{256}Fm, which was measured with a neutron-detection efficiency of only 31%, $\bar{\nu}_T$ was normalized to the reported value[6] of $\bar{\nu}_T = 3.73 \pm 0.18$. The distribution was not unfolded because of the low detection efficiency, but the variance $\sigma_{\nu_T}^2$ was calculated from the relationship:

$$\sigma_{\nu_T}^2 = \epsilon^{-2}(\sigma_d^2 - \sigma_b^2) + \epsilon^{-1}(1-\epsilon^{-1})(\bar{\nu}_d - \bar{\nu}_b). \quad (3)$$

Our value of 1.82 ± 0.08 is smaller than the reported value[6] of 2.30 ± 0.65, but is within the quoted uncertainties. Our value of Γ_2 of 0.863 is also somewhat smaller than the reported value.

Figures 5–8 show the unfolded distributions $P_t(\nu)$ as a function of mass fraction and TKE for ^{250}Cf, ^{252}Cf, ^{254}Cf, and ^{257}Fm. Figure 9 shows $P_t(\nu)$ for all fragment masses as a function of TKE and Fig. 10 shows $P_t(\nu)$ for all TKE's as a function of fragment masses. The values of $\bar{\nu}$, σ_ν^2, and Γ_2 are given in Tables II through V. Although the unfolded $P_t(\nu)$ distributions could not be derived for ^{256}Fm because of the low efficiency of the measurement, values of $\bar{\nu}$, σ_ν^2, and Γ_2 could still be calculated as a function of mass and TKE and are given in Table VI. (For purposes of display in Figs. 5–10, categories containing ≤ 50

TABLE VI. Means and variances of the neutron multiplicity distributions of ^{256}Fm (47 366 fission events).

	Mass numbers derived from mass ratios				
	128.0–138.2 128.0–117.8	138.2–148.5 117.8–107.5	148.5–158.7 107.5–97.3	158.7–169.0 97.3–87.0	All mass numbers
220–240 MeV					
SF[a]	2 260	451			2 712
$\bar{\nu}$	1.98	1.51			1.90
σ_ν^2	1.15	0.96			1.15
Γ_2	0.788	0.759			0.792
200–220 MeV					
SF[a]	8 047	7 088	629		15766
$\bar{\nu}$	3.29	2.80	2.01		3.02
σ_ν^2	1.67	0.56	0.51		1.22
Γ_2	0.850	0.714	0.629		0.803
180–200 MeV					
SF[a]	5 214	11 944	4617	337	22 119
$\bar{\nu}$	4.53	4.05	3.43	2.95	4.01
σ_ν^2	2.18	0.49	0.88	0.69	1.12
Γ_2	0.885	0.783	0.783	0.704	0.820
160–180 MeV					
SF[a]	760	2 414	2424	626	6 263
$\bar{\nu}$	5.69	5.30	4.69	4.45	5.01
σ_ν^2	0.92	1.26	0.20	2.59	1.19
Γ_2	0.853	0.856	0.796	0.906	0.849
All energies					
SF[a]	16 362	21 899	7671	965	46 943
$\bar{\nu}$	3.60	3.73	3.71	3.92	3.73 ± 0.18[b]
σ_ν^2	2.65	1.31	1.31	2.40	1.82 ± 0.08
Γ_2	0.927	0.826	0.827	0.901	0.861

[a] Number of fission events in the specified energy and mass ranges.
[b] Reference 6.

events are not shown.) Calculated standard deviations for $\bar{\nu}$, σ_ν^2, and Γ_2 for several cases with different numbers of observed SF events are shown in Tables II and III. (The standard deviations for Γ_2 were calculated using the appropriate correlation coefficients derived from the unfolding procedure.) These given an idea of the statistical errors involved for the other cases presented here.

From our measurements of the kinetic energies of coincident fragments and the emitted neutrons, the TKE, mass fraction (M_H/A) for the fragments, and the average total number of neutrons per fission event can be derived. However, we cannot tell how many of these neutrons were emitted from the light and how many from the heavy fragment. Therefore, in Figs. 5–10 and in Tables II–IV, we give the mass range of both fragments for each group of events.

The $\bar{\nu}$ values for all five nuclides decrease monotonically with increasing TKE for a given mass split. This might be expected since the total energy is approximately constant for a given mass split and is manifested primarily either in the kinetic or excitation energy of the fragments. Thus, as the TKE increases, the excitation energy of the fragments, and hence the energy available for emission of neutrons (and photons), must necessarily decrease. In the case of ^{257}Fm, $\bar{\nu}$ drops to 1.08 and 0.80, respectively, for symmetric and near-symmetric mass splits for the highest TKE groups, while for the other nuclides $\bar{\nu}$ drops only to 1.96 and 1.36. This difference may be a result of the fact that the TKE for symmetric and near-symmetric mass splits for ^{257}Fm reaches values some 50 to 30 MeV higher (see Fig. 11) than for the other nuclides shown, even though the estimated Q value[9,10] for ^{257}Fm is nearly the same as for ^{256}Fm and only about 15 MeV higher than for the Cf isotopes. The contour plots of TKE as a function of mass fraction for ^{254}Cf, ^{256}Fm, and ^{257}Fm shown in Fig. 11 illustrate the difference in TKE release and its variance for different mass fractions for these nuclides. ^{257}Fm exhibits much larger spreads in TKE for symmetric mass division than the other nuclides. These differences in TKE in the region of symmetric mass division

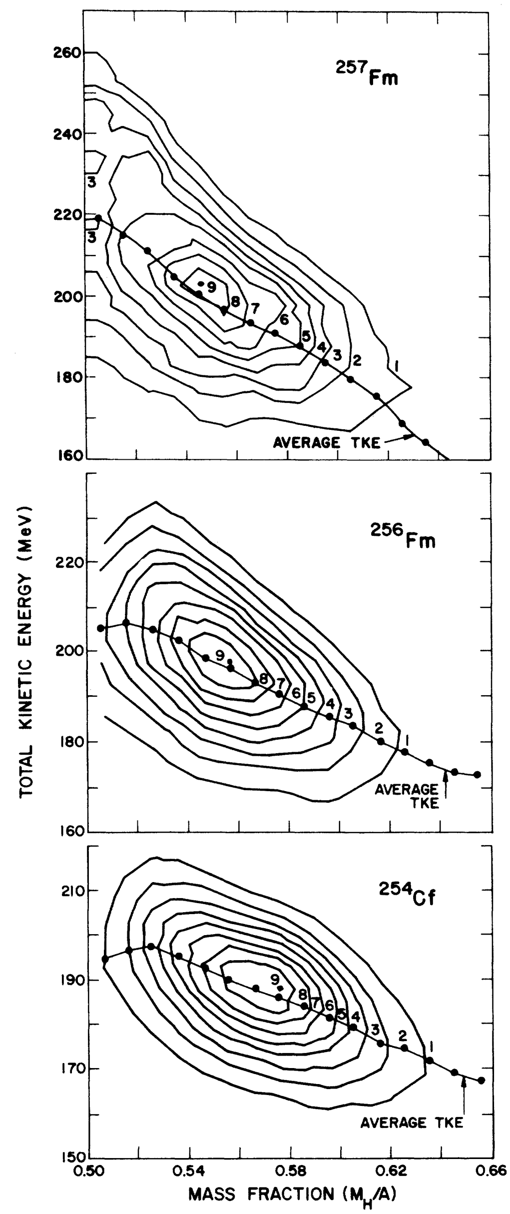

FIG. 11. Contour diagrams showing pre-neutron-emission TKE distributions as a function of mass fraction for ^{254}Cf, ^{256}Fm, and ^{257}Fm (data for ^{257}Fm from Ref. 1.) The contours are lines of relative numbers of events, based on data groupings 5 MeV × 0.01 units of mass fraction.

(M_H/A = 0.50 to 0.54) may be due to the approach of the symmetric fragments from SF of ^{257}Fm to the spherical, doubly magic ^{132}Sn configuration for which the Coulomb repulsion, and hence the TKE, should reach a maximum value. (^{256}Fm shows this effect to a lesser degree.) The highest TKE group summed over all mass splits, as shown in Tables II–VI and Fig. 9, shows the lowest neutron emission for all these nuclides, 1.07 to 2.15. The lowest TKE group shows the highest values, $\bar{\nu}$ = 4.51 to 5.38. Thus, $\bar{\nu}$ changes from 1.07 to 5.38 as a function of TKE, but changes only from 3.13 to 4.09 for the various mass groups summed over all TKE's (Tables II–VI and Fig. 10.)

For the lowest TKE groups, $\bar{\nu}$ is typically 1 or 2 neutrons less for asymmetric fissions than for symmetric fissions (see Tables II–VI and Figs. 5–8). Although the Q values decrease by about 35 to 40 MeV as the mass fraction increases from 0.52 to 0.66, the decrease in Q is apparently not completely accounted for by the observed decrease in neutron emission. Since constraining the TKE to low values at symmetry selects the more highly distorted fragments, perhaps more of the energy is dissipated by photon emission for the low-energy, near-symmetric mass splits.

The mass yield for ^{257}Fm SF events with TKE >235 MeV, where $\bar{\nu}$ is only about 1, is shown in Fig. 12. This mass distribution resembles those measured[11,12] for SF of ^{258}Fm and ^{259}Fm where the most probable TKE's are 238 and 242 MeV, respectively, and suggests that neutron emission may also be low for ^{258}Fm and ^{259}Fm. This is further supported by the fact that their TKE's are approaching the Q values of 250 to 255 MeV estimated for symmetric fission from mass

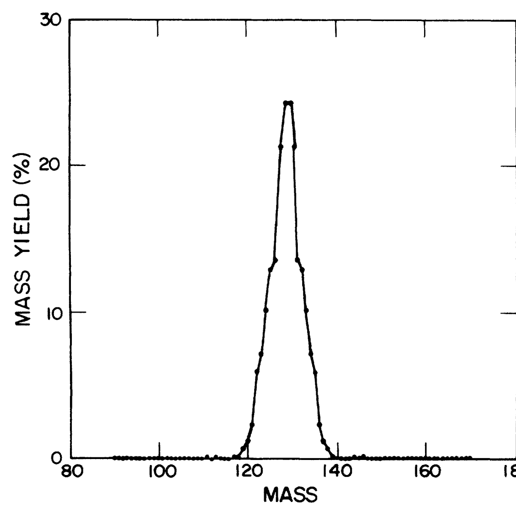

FIG. 12. Mass-yield distribution for ^{257}Fm for fission events with TKE > 235 MeV.

tables.[9,10]

The large variances observed for neutron emission from ^{256}Fm and ^{257}Fm (Table I, Fig. 4) suggest a broad distribution in fragment excitation energies. This may perhaps be attributed to the fact that these nuclides are in a "transition" region, i.e., although symmetric fragments can have the magic proton number of 50, they are still 3 to 4 neutrons from the 82-neutron closed-shell configuration. The fragments may then be rather "soft" to deformation, and the observation of symmetric fragments with both very high and very low TKE indicates a rather large difference in their shapes, ranging from elongated to nearly spherical.

The number of neutrons emitted per fission and the variance should decrease very sharply for ^{258}Fm and ^{259}Fm and higher mass fermium isotopes as symmetric mass division results in fragments which more closely approach the rigid doubly magic configuration. If this hypothesis is correct, then neutron emission and its variance might be expected to increase again for fissioning systems with Z greater than 100.

This work was performed under the auspices of the U.S. Department of Energy.

[1]J. P. Balagna, G. P. Ford, D. C. Hoffman, and J. D. Knight, Phys. Rev. Lett. 26, 145 (1971).
[2]J. P. Balagna, J. A. Farrell, G. P. Ford, A. Hemmendinger, D. C. Hoffman, L. R. Veeser, and J. B. Wilhelmy, *Proceedings of the Third International Atomic Energy Symposium on the Physics and Chemistry of Fission, Rochester, 1973* (IAEA, Vienna, 1974), Vol. II, p. 191.
[3]D. C. Hoffman and M. M. Hoffman, Annu. Rev. Nucl. Sci. 24, 151 (1974).
[4]L. R. Veeser, E. D. Arthur, and P. G. Young, Phys. Rev. C 16, 1792 (1977); L. R. Veeser, *ibid.* 17, 385 (1978).
[5]J. W. Boldeman, in *Neutron Standard Reference Data* (IAEA, Vienna, 1974), p. 291.
[6]Yu. A. Lazarev, At. Energy Rev. 15, 75 (1977).
[7]C. J. Orth, Nucl. Sci. Eng. 43, 54 (1971).
[8]B. C. Diven, H. C. Martin, R. F. Taschek, and J. Terrell, Phys. Rev. 101, 1012 (1956).
[9]P. A. Seeger and W. M. Howard, Los Alamos Scientific Laboratory Report No. LA-5750 (1974); A. H. Wapstra and K. Bos, At. Data Nucl. Data Tables 17, 474 (1976).
[10]W. D. Myers, *Droplet Model of Atomic Nuclei* (IFI/Plenum, New York, 1977).
[11]E. K. Hulet, R. W. Lougheed, J. H. Landrum, J. F. Wild, D. C. Hoffman, J. Weber, and J. B. Wilhelmy, *Transplutonium 1975, Proceedings of the 4th International Transplutonium Element Symposium* (North-Holland, Amsterdam, 1976), p. 353; D. C. Hoffman, J. Weber, J. B. Wilhelmy, E. K. Hulet, J. H. Landrum, R. W. Lougheed, and J. F. Wild, *Proceedings of the 3rd International Conference on Nuclei Far from Stability, Cargèse, 1976* (CERN, Geneva, 1976), p. 558.
[12]D. C. Hoffman, J. B. Wilhelmy, J. Weber, and W. R. Daniels, LASL; E. K. Hulet, J. H. Landrum, R. W. Lougheed, and J. F. Wild, LLL, Los Alamos Scientific Laboratory Report No. LA-UR-77-2901 (1977).